Transmission of Elegant Laguerre-Gaussian beams at a dielectric interface – numerical simulations

W. SZABELAK and W. NASALSKI[*]

Institute of Fundamental Technological Research, Polish Academy of Sciences, 21 Świętokrzyska St., 00-049 Warsaw, Poland

Abstract. Behaviour of Laguerre-Gaussian beams impinged at a dielectric interface under distinct angles is discussed. For different incident angles the beams interact with the interface differently. Two ranges of incident angles, specified by a position of a spectral cone of beam field and related to a cross-polarization effect, are analyzed. Boundary between these two ranges is defined. Cases of critical incidence and total internal reflection are also discussed. Paraxial beams near the lower paraxial limit are considered. Theoretical predictions are confirmed by numerical simulations.

Key words: oblique incidence, transmission, cross-polarization, optical vortices, paraxial beams, Elegant Laguerre-Gaussian beams.

1. Introduction

The subject of optical beams at a dielectric surface was under intense studies since the beginning of the last century. Extensive summary of the problems can be found in Ref. [1] together with numerus references. We consider mainly one aspect of the problem – behaviour of optical vortices at a dielectric interface. Optical vortices are characteristic ingredients of the Elegant Laguerre-Gaussian (ELG) beams and their the well-defined spin and orbital angular momentum [2–5]. In this contribution the beam-interface interactions are discussed in the context of their dependence on an incidence angle of the ELG beams. For different incidence angles the beams interact with the interface differently.

In the case of normal incidence, an azimuthal index of a reflected or transmitted ELG beam is increased or decreased by the cross-polarization coupling in the beam component orthogonal (opposite) to the polarization component of the incident beam [5]. Let us call this phenomenon as the "normal" vortex excitation. The case of oblique incidence, however, appears to be different. One can consider the beam field distribution only in the first-order approximation with respect to an azimuthal angle defined in the interface plane [6]. The azimuthal angle selects the spectral component of the substantial beam amplitude what entails the dependence of the optical vortex excitation on the incident angle. A specific value of the incident angle can be associated with an upper limit of the range where the "normal" excitation of higher-order beam modes in the opposite component may be taken as valid.

The transition from the normal incidence range to the oblique incidence range may be roughly understood as the diminishing of the "normal" vortex excitation in the opposite beam component. For the ELG beams, the wave vectors of the main (the most intense) spectral components form a cone of cylindrical symmetry. One slant height of the cone represents one wave vector. The boundary between the normal and oblique incidence ranges can be referred to the situation, when one of the slant heights of the cone becomes normal, that is, when this spectral component of the beam propagates perpendicularly to the interface. In this case the range of azimuthal angle corresponding to the ensemble of spectral components of substantial amplitudes decrease twice. This finally results in the domination of the g-o contribution in the opposite beam component.

In Sec. 2 theoretical background of the problem is presented. Transmission of the ELG beams are analyzed in Sec. 3. In Sec. 4 conclusions are presented. Short note about vortex excitation under normal incidence is given in Appendix A.

2. Beams at a dielectric interface

In this section we give a few basic equations necessary for future interpretation of numerical results. Derivation of this equations can be found in Ref. [5]. In Subsec. 2.1 the beam-interface interrelation described in the cylindrical polarization basis (CR, CL) is presented. Decomposition of the ELG beams in the spectral domain is given in Subsec. 2.2. Short analysis of the action of the interface is presented in Subsec. 2.3.

2.1. Theoretical background. It is convenient to consider the spectral components of the ELG beams as the plane waves propagating at different azimuthal φ and polar ϑ angles. The interface frame *OXYZ* and three *Oxyz* reference frames, for the incident, transmitted and reflected beams are presented in Fig. 1. To find amplitudes and transmission coefficients for all spectral components in one reference frame, here in the interface frame *OXYZ*, we need to use two rotations for each of them: first about Y-axis by ϑ and second about Z-axis by φ. Details of this computation are presented in Ref. [5] and will

*e-mail: wnasal@ippt.gov.pl

not be recalled here. Generally, we can write the beams spectral components in the linear polarization basis (*TM, TE*) as

$$\widetilde{\underline{E}}^{(b)} = \widetilde{\underline{E}}_X^{(b)} \underline{e}_X + \widetilde{\underline{E}}_Y^{(b)} \underline{e}_Y, \qquad (1)$$

where $\underline{e}_X$, $\underline{e}_Y$ are the beam polarization vectors, $\widetilde{\underline{E}}^{(b)}$ is the amplitude vector for the incident $(b = i)$, transmitted $(b = t)$ and reflected $(b = r)$ fields. The relation between the transmitted and incident spectral components is given by

$$\widetilde{\underline{E}}^{(t)} = \underline{\underline{t}}_{(X,Y)} \widetilde{\underline{E}}^{(i)}, \qquad (2)$$

where $\underline{\underline{t}}_{X,Y}$ is the transmission matrix. Its counterpart in circular polarization basis (CR, CL) is given by [5]

$$\underline{\underline{t}}_{(R,L)} = \frac{1}{2} \left(\eta t_p + t_s \right) \begin{bmatrix} 1 & 0 \\ 0 & 1 \end{bmatrix} +$$

$$+ \frac{1}{2} \left(\eta t_p - t_s \right) \begin{bmatrix} 0 & \exp\left[-2i\varphi\right] \\ \exp\left[+2i\varphi\right] & 0 \end{bmatrix}, \qquad (3)$$

where $\eta = \cos \Theta^{(t)} / \cos \Theta^{(i)}$ and $t_p \equiv t_p(\vartheta_i)$, $t_s \equiv t_s(\vartheta_i)$ are the Fresnel coefficients. The two terms above are the two 2×2 matrices corresponding to the direct (DP) and cross (XP) polarization effects, respectively.
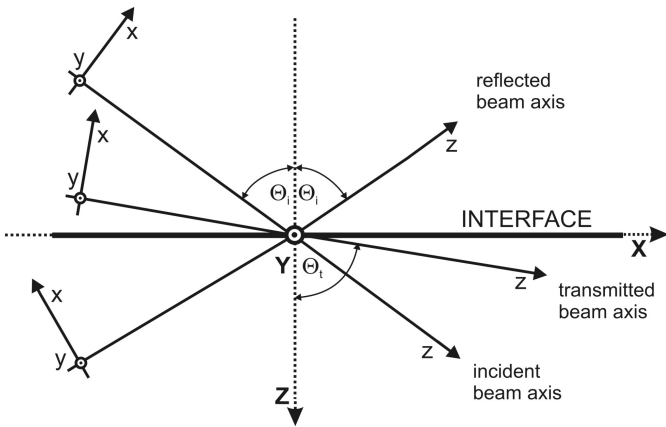

Fig. 1. Interface $OXYZ$ and beam $Oxyz$ reference frames for the incident, transmitted and reflected beams

For clarity of further considerations we can rewrite the terms placed before the square brackets in (3) as

$$t_{(DP)} = \frac{1}{2} \left(\eta t_p + t_s \right),$$

$$t_{(XP)} = \frac{1}{2} \left(\eta t_p - t_s \right). \qquad (4)$$

As they are 3D counterparts of the standard (2D) Fresnel coefficients, let us call them as modified spectral coefficients. Figure 2 depicts them versus normalized spectral variable $k_\perp / k_i$.

Let us now consider more closely the optical beam field on which the transmission matrix (3) can be applied.
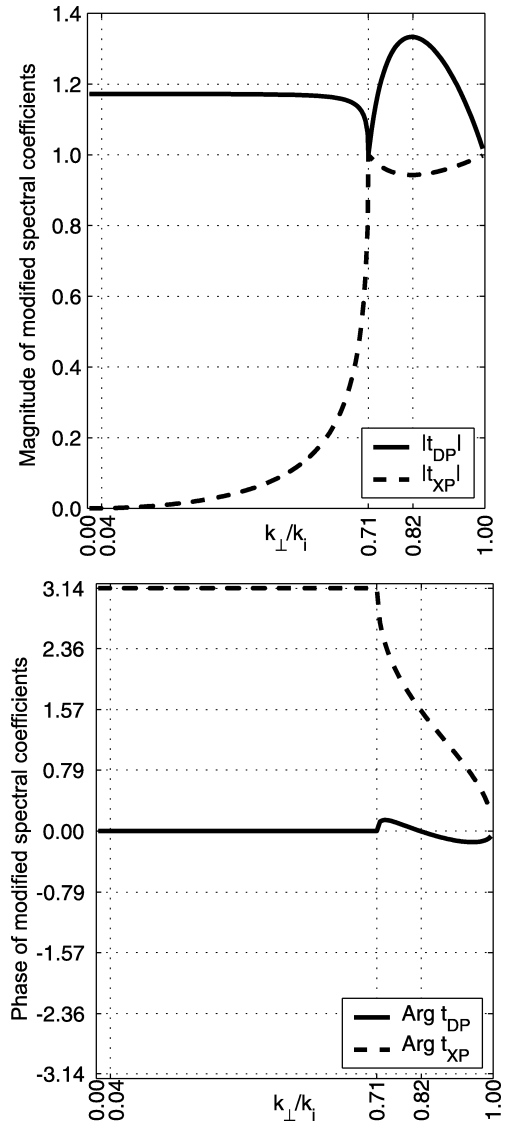

Fig. 2. Magnitude (top) and phase (bottom) of the 3D counterparts of the standard (2D) Fresnel coefficients in the internal case (a critical angle is 45°) versus $\sin \vartheta_i = k_\perp / k_i$. Black solid curve is for t_{DP}, dashed for t_{XP}. Three values on the axis of abscissa, 0.04, 0.71, 0.82 are for "significant" $(\cong 2°, k_i w_w = 10 \cdot 2\pi$, see Subsec. 3.2), critical (45°, Subsec. 3.3) and TIR (55°, Subsec. 3.4) regions of the incident angle, respectively

2.2. Elegant Laguerre-Gaussian beams in the spectral domain.
General form of the beam field in the spectral domain has been presented in the previous section. Here we give explicit forms of the ELG beams. The harmonic dependence on time $\exp[-i\omega t]$ and a propagation distance $\exp[ik^{(b)}z]$ are assumed and suppressed.

In the spatial domain all higher-order modes of the ELG beams can be derived by acting with differential operators on fundamental Gaussian mode. Corresponding spectral operators are simply the algebraic multiplication of the spectral amplitudes instead [5, 7–9]. Then, the form of ELG beams in the spectral domain is given by

$$\widetilde{G}_{p,l}^{(EL)} \left(\kappa, \bar{\kappa}, z \right) \sim \left(i w_w \right)^{2p+l} \kappa^{p+l} \bar{\kappa}^p \tilde{G} \left(\kappa, \bar{\kappa}, z \right), \qquad (5)$$

where $\kappa = 2^{-1/2}(k_x + ik_y)$ and the overbar means complex conjugate. The spectral Gaussian function $\widetilde{G}(\kappa, \bar{\kappa}, z) = 2\pi \exp[-\kappa\bar{\kappa}v^2]$ is given by the complex beam half-width (radius) $v^2 = w_w^2 (1 + izz_D^{-1})$ with the diffraction length of a beam $z_D = k_i w_w^2$ and beam (real) half-width at the waist w_w. The CR polarized ELG beam field is represented by $\underline{\widetilde{E}} = \widetilde{G}_{p,l}^{(EL)} \underline{e}_R$.

For convenience of further considerations let us look closer to the spectral form of ELG beam – Eq. (5). It is easy to predict the beam amplitude at the plane $z = 0$. Consider the surface represented by $|\kappa^{p+l}\bar{\kappa}^p|$ in spectral coordinates k_x, k_y. It is described by the equality $|\kappa^{p+l}\bar{\kappa}^p| \cong k_{ro}^{2p+l}$, where $k_{ro}^2 = k_x^2 + k_y^2$. If we multiply fundamental Gaussian function by $\kappa^{p+l}\bar{\kappa}^p$, we will obtain one ring with finite width in amplitude distribution. The maximum of this ring (let us call it spectral ring) represents the ensemble of the main spectral components (the most intense). The normalized radius of spectral ring $(k_r w_w)$, defined by a position of a field maximum, depends on the order $(N = 2p + l)$ of the ELG beam and is given by

$$k_r w_w = \sqrt{N}. \tag{6}$$

We can build a spectral cone of the ELG beam in the similar way as spectral cones of Bessel-Gaussian beams described in Ref. [10]. The spectral ring forms a base of the cone. All wave vectors of main spectral components represent the slant heights of the cone. Longitudinal components $(k_z^{(i)})$ of wave vectors are constant for all main components and form a height of the cone. Direction of this height is in accordance with direction of beam propagation. The spectral cones, for different incident angles, are depicted in Sec. 3.

Numerical simulations consist mainly in the use of transmission matrix (3). To make transposition from the spectral domain to the spatial domain we use the fast Fourier transform algorithm. In the next subsection the action of the interface on the incident ELG beam is analyzed by use of transmission matrix.

2.3. Action of the interface. Consider the ELG beam incident upon the dielectric interface. In the case of normal incidence, on the grounds of Eqs. (3) and (5), we can describe the action of the interface by [5]:

$$\begin{bmatrix} \widetilde{E}_R^{(t)} \\ \widetilde{E}_L^{(t)} \end{bmatrix}_{CR} = t_{DP} \begin{bmatrix} \widetilde{G}_{p,l}^{(EL)} \\ 0 \end{bmatrix} + t_{XP} \begin{bmatrix} 0 \\ \widetilde{G}_{p-1,l+2}^{(EL)} \end{bmatrix}, \tag{7}$$

$$\begin{bmatrix} \widetilde{E}_R^{(t)} \\ \widetilde{E}_L^{(t)} \end{bmatrix}_{CL} = t_{DP} \begin{bmatrix} 0 \\ \widetilde{G}_{p,l}^{(EL)} \end{bmatrix} + t_{XP} \begin{bmatrix} \widetilde{G}_{p+1,l-2}^{(EL)} \\ 0 \end{bmatrix}, \tag{8}$$

where the labels CR and CL indicate the type of polarization of the incident beam. The excitation and annihilation of the optical vortices in the beam opposite component are now clearly visible. For different polarization cases the topological charge l changes differently. It increases (decreases) by 2 for CR (CL) polarization of the incident beam, meanwhile the radial index p decreases (increases) by 1.

In the case of oblique incidence a diameter of the range of azimuthal angles decreases. It results in the geometrical optics domination of the whole process. This aspect of beam transmission will be discussed below.

3. Elegant Laguerre-Gaussian beam incidence

In this section we consider the beam incidence under various incident angles. In all of them, the incident beam is ELG with $p = 1$, $l = 3$ (Fig. 3) of CR polarization, which propagates in the optically denser medium (the critical angle is $\Theta_C = 45°$). Normalized width of the beam is $k_i w_w = 10 \cdot 2\pi$. This is within the paraxial range, near the lower paraxial limit. The transverse field is defined in the plane perpendicular to the beam propagation direction ($k_z = $ const). It results in elliptic character of the field amplitude at the interface plane. Angles of incident beam are special chosen. Apart from critical incidence, in all other cases the spectral derivatives ($\partial_{k_\perp}$) of the magnitude of the modified spectral components are close to their zeroes, see their values on axis of abscissa in Fig. 2.
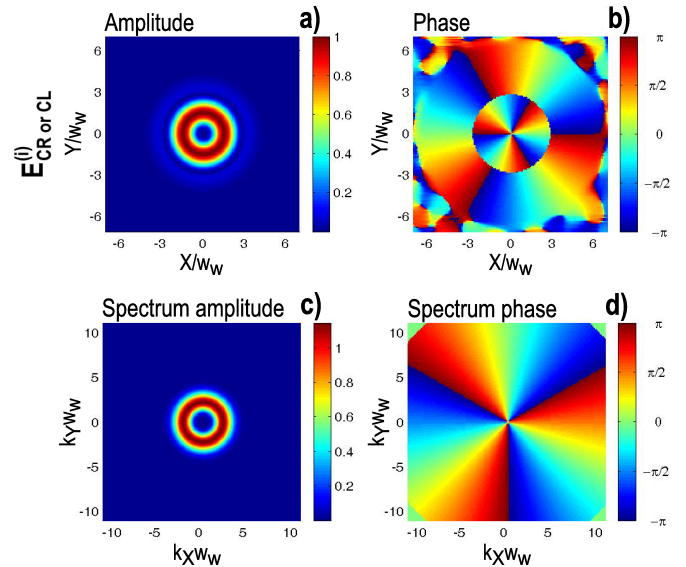

Fig. 3 (colour online). Spatial, (a)–(b), and spectral, (c)–(d), decompositions of the incident ELG beam, $p = 1$, $l = 3$ versus normalized coordinates in the case of normal incidence. Note that for the case of oblique incidence these decompositions stay valid when $k_X \to k_x$, $k_Y \to k_y$

It is important to note that the numerical simulations were obtained by use of the matrix representation of the problem. In various incident angle (Θ_i) cases the range of azimuthal (φ) and polar (ϑ) angles is different. This entails the qualitatively distinct action of the interface, governed by the transmission matrix (3).

Note that in the next subsections we use some arrangement of figures that show transmitted field decompositions. In each subsection are two figures. The first depict spectral incident cone in $Ok_X k_Y k_Z$ frame and also, in the next subplot, the spectral ring with magnitude of modified spectral component $|t_{XP}|$ in the plane of the interface along k_X coordinate. For convenience the spectral cone and ring are scaled. The spectral cone is wider, whereas the spectral ring is scaled to have its maximum equal to 0.6. The second figure shows the decomposition of the transmitted components with, mutual

for each subsection, arrangement of the rows: the first two are for the DP polarization component, the second two – for the XP polarization component. For the beam incident angles greater than critical, the decomposition of the transmitted beam represents the evanescent field below the interface. Note that in all presented cases of incidence, apart from that of critical, the total amplitude distribution of the transmitted field is similar to the DP transmitted component.

3.1. Range of normal incidence. In Subsec. 2.2 we described the spectral cone of the ELG beam. In the normal incidence case the height of the cone is perpendicular to the interface. The incident reference frame $Oxyz$ coincides with the interface frame $OXYZ$. This means that the range of azimuthal angles, which specify main spectral components, is equal in k_x-k_y and k_X-k_Y planes and amounts $|\varphi| \leq \pi$, see Fig. 4a. The zero point between two peaks of the spectral ring in Fig. 4b is exactly at zero position corresponding to normal incidence.
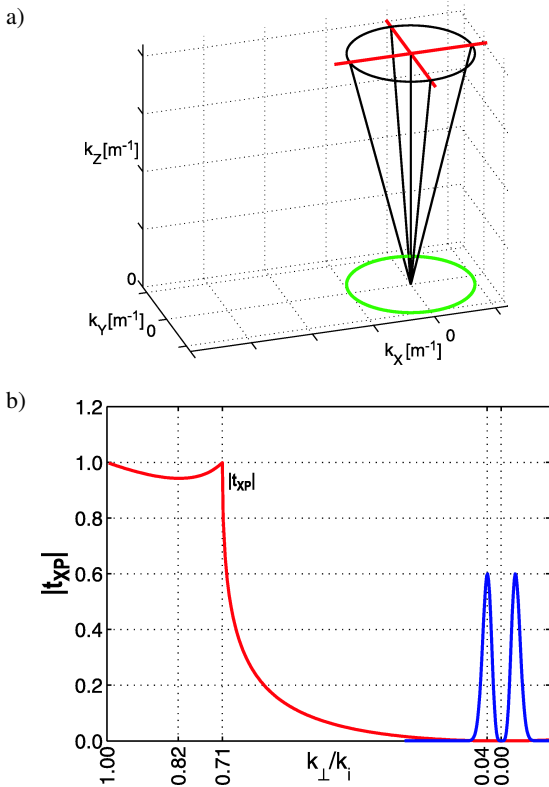

Fig. 4 (colour online). Spectral cone under normal incidence a), and magnitude of t_{XP} in the spectral domain (red solid curve) with the spectral ring of the ELG beam (blue solid curve) (b). The red lines on (a) correspond to k_x and k_y, four slant heights to the wave vectors of four main components, the black (green) circle to the spectral ring in k_x-k_y (k_X-k_Y) plane. Note that the range of azimuthal angles is $(-\pi,\pi]$. The peak positions of the spectral ring on (b) are specified for the ELG beam, $p = 1$, $l = 3$, $k_i w_w = 10 \cdot 2\pi$. Peak's hight is scaled to 0.6. Values on the axis of abscissa have the same meaning as in Fig. 2.

Figure 5 shows the action of the interface. Let us look closer to the opposite component. The topological charge l increases by 2 as shown in Eq. (7). Moreover, the radial index

p decreases by 1. But the amplitude of t_{XP} is also dependent on the incident angle ϑ_i. From the numerical simulations it may be inferred that this dependence, in the vicinity of normal incidence, additionally increases the radial index by one. Then it seams that the decomposition of the amplitude and phase, (e) and (f), may correspond to $G_{p,l+2}^{(EL)}$ (see Appendix A for additional comments on this problem). Details of the normal incidence were analyzed theoretically and numerically in Ref. 5. Our results given here confirm that analysis.
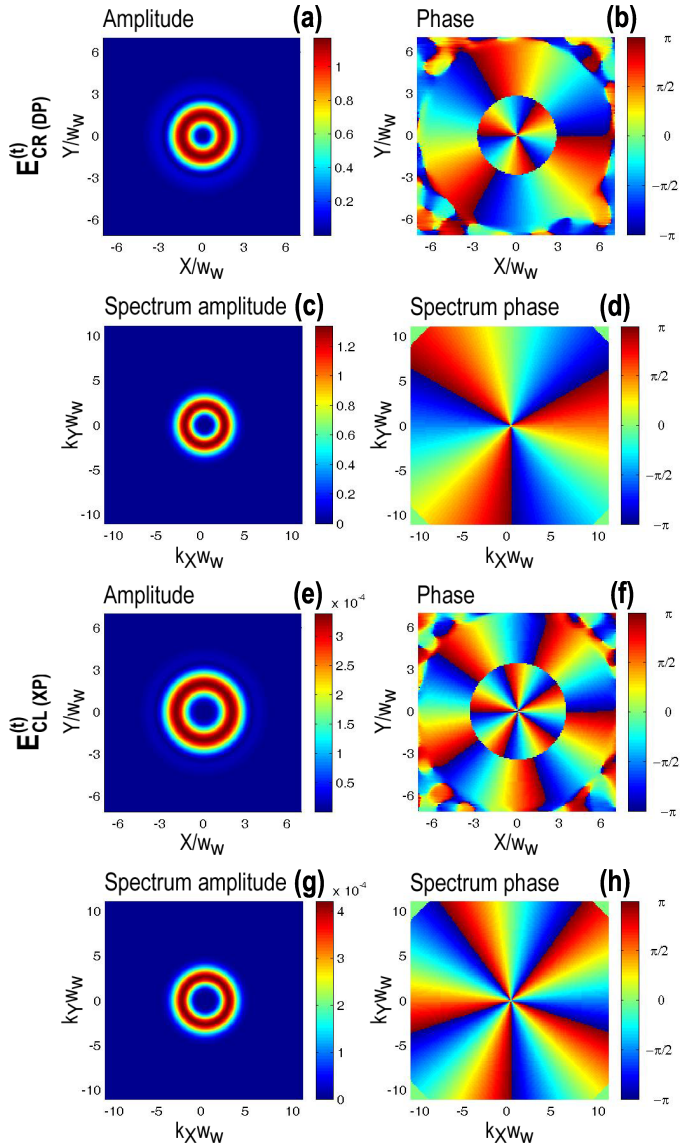

Fig. 5 (colour online). Transmitted filed components in the case of normal incidence of the ELG beam, $p = 1$, $l = 3$, $k_i w_w = 10 \cdot 2\pi$, CR (see Fig. 3). The first two rows represent the direct polarization component. Excitation of the optical vortices and change of the topological charge are clearly visible in the opposite component in the second row. The first and second column are respectively the amplitude and phase decompositions in the spatial and spectral domains. The third and fourth rows show the amplitude and phase of spectral components. (a)–(d) the CR (DP) component of transmitted beam, (e)–(h) the CL (XP) component of transmitted beam. The amplitude of total transmitted field (is not shown here) is similar to the DP component.

3.2. Significant incident angle. If we increase the incident angle enough, we will obtain a situation when one of the slant height of the inclined cone will be normal to the interface (see Fig. 6a).
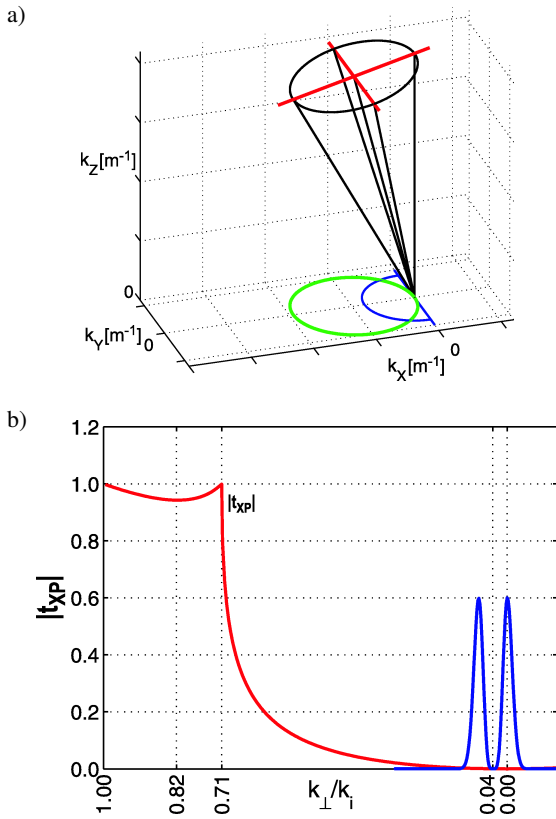
a)

b)

Fig. 6 (colour online). Spectral cone under the "significant" incidence ($\Theta_i = \Theta_S \cong 2°$) (a), and magnitude of t_{XP} in the spectral domain (red solid curve) with the spectral ring of the incident ELG beam $p = 1$, $l = 3$, $k_i w_w = 10 \cdot 2\pi$ (blue solid curve) (b). Meanings of the lines and curves are the same as in Fig. 4. Now, the cone is inclined and the spectral ring peaks are shifted by $\sin \Theta_S$. The range of azimuthal angles has been changed into $(-\pi/2, \pi/2)$, see blue half-circle in (a).

In this case the range of azimuthal angles in the plane k_X-k_Y decreases sharply from $|\varphi| \leq \pi$ to $|\varphi| \leq \pi/2$ (see blue half-circle in k_X-k_Y plane in Fig. 6a). The "significant" case is defined as the boundary between the normal and oblique incident ranges, as upper border of "normal" vortex excitation. Note that the "significant" angle can be easily computed. It is the angle between height and slant height of the cone. Thus:

$$\sin \Theta_S = \frac{k_r}{k_i} = \frac{\sqrt{N}}{k_i w_w}. \qquad (9)$$

The decomposition of the two orthogonal, transmitted beam components in the spatial and spectral domain is shown in Fig. 7. A half-moon in the spectral domain is now vivid as the result of the one of main spectral components specified by $\vartheta_i = 0°$. The modified spectral coefficient $t_{XP}(\vartheta_i = 0°) = 0$. The cross-polarization does not exist for the spectral component normal to the interface. See the position of the spectral

ring peak for this component in Fig. 6b. It is exactly placed at zero position. For the components that satisfy $\vartheta_i > 0°$ $t_{XP} \neq 0$. It is responsible for non zero part of the half-moon.
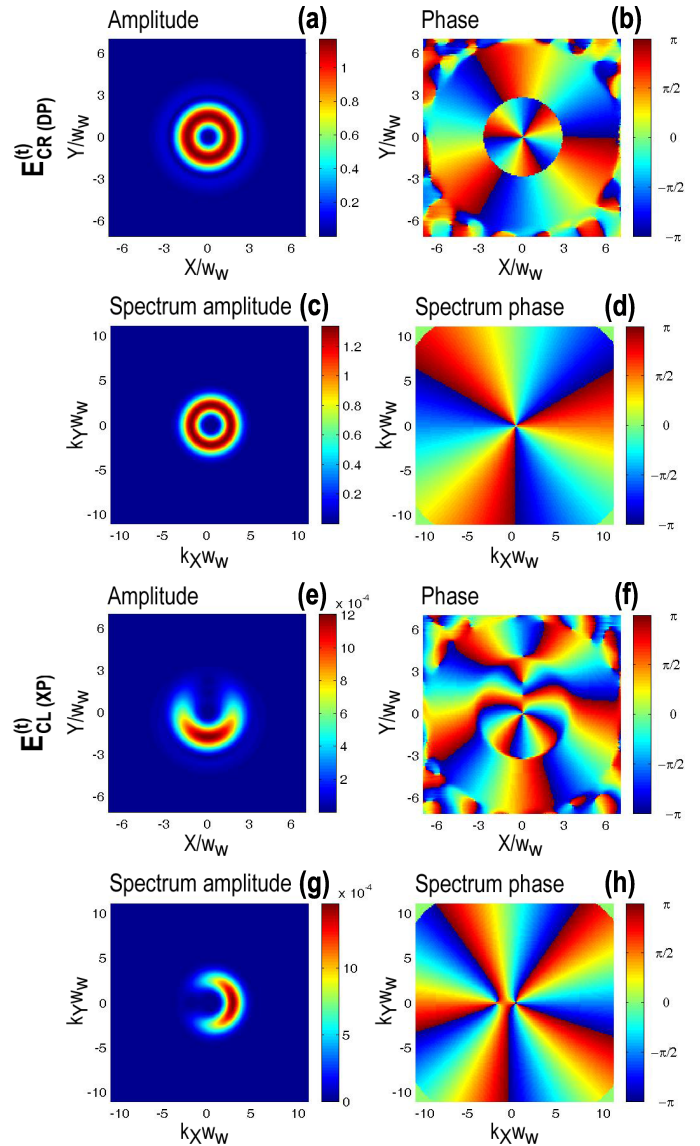

Fig. 7 (colour online). Transmitted components of the CR incident ELG beam, $p = 1$, $l = 3$ (see Fig. 3) in the case of the "significant" incidence, $\Theta_i = \Theta_S \cong 2°$ for $k_i w_w = 10 \cdot 2\pi$. The two first (second) rows show the DP (XP) component of the transmitted beam. The first and second column are respectively the amplitude and phase decompositions in the spatial and spectral domains. The third and fourth rows show the amplitude and phase of spectral components. Values on the axis of abscissa are shown with reference to the global shift $k_i w_w \sin \theta_i$. (a)–(d) the CR (DP) component of transmitted beam, (e)–(h) the CL (XP) component of the transmitted beam. The amplitude of the total transmitted field (is not shown here) is similar to the DP component.

3.3. Critical incidence. The case of critical incidence is rich in different physical phenomena, e.g. the nonspecular effects of reflection [11, 12], the presence of evanescence of the transmitted field and so on. The standard Fresnel coefficients and

their 3D counterparts (Eq. (4)) possess singularities exactly in the critical angle. Meanwhile the critical incidence means that roughly half of all spectral components of the 3D beams undergo the total internal reflection, the second half of components does not and is connected to the purely real modified spectral coefficients (see Figs. 8b and 2).
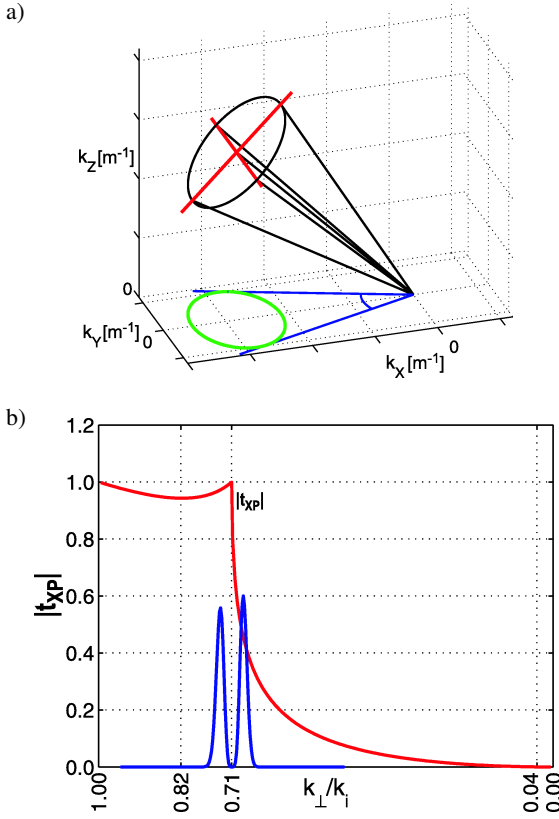
a)

b)

Fig. 8 (colour online). Spectral cone in the case of critical incidence ($\Theta_i = \Theta_C = 45°$) (a), and magnitude of t_{XP} in the spectral domain (red solid curve) with the ring of the incident ELG beam $p = 1$, $l = 3$, $k_i w_w = 10 \cdot 2\pi$ (blue solid curve) (b). Meanings of the lines in (a) are the same as in Fig. 4. The cone is inclined and the spectral ring peaks are shifted by $\sin(\Theta_i = 45°)$. Note that the range of azimuthal angles is less then $(-\pi/2, \pi/2)$, see blue circular sector in (a).

Apart from singularities of spectral coefficients, it is also one thing important to note. Under oblique incidence (in the case when $\Theta_i > \Theta_S$) the range of azimuthal angles that selects substantial spectral components is less than $(-\pi/2, \pi/2)$ (see blue circular sector in k_X-k_Y plane in Fig. 8a). That entails domination of the geometrical optics but does not blur strong effects caused by the critical incidence. Subsec. 3.4 presents oblique incidence when the domination of the geometrical optics is clearly visible and is not distorted by the critical incidence phenomena.

Keeping in mind the position of the spectral peaks and the form of the modified spectral coefficients shown in Figs. 8b and 2, see decomposition of the transmitted fields shown in Fig. 9. Let us start our consideration from the spectral domain. First, in the direct polarization component (c)–(d) nothing
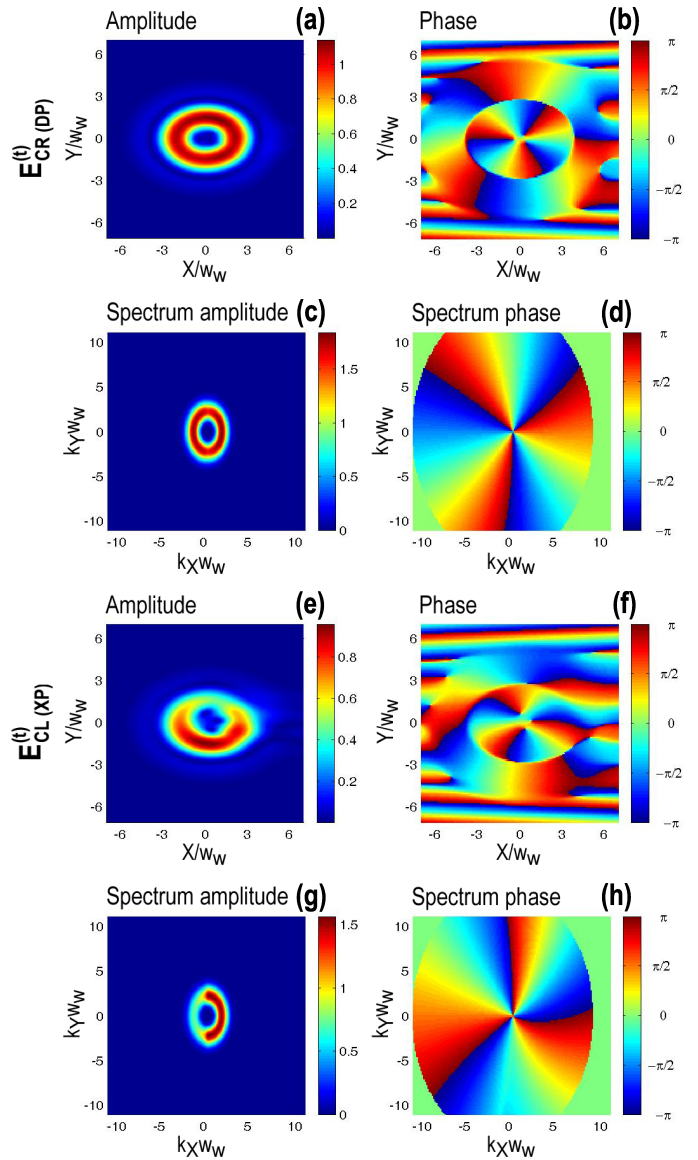

Fig. 9 (colour online). Transmitted components of the CR incident ELG beam $p = 1$, $l = 3$, $k_i w_w = 10 \cdot 2\pi$ (see Fig. 3) in the case of the critical incidence. The first two (second) rows show the DP (XP) component of the transmitted beam. The first and second column are respectively the amplitude and phase decompositions in the spatial and spectral domains. The third and fourth rows show the amplitude and phase of spectral components. Values on the axis of abscissa are shown with reference to the global shift $k_i w_w \sin \theta_i$. (a)–(d) the CR (DP) component of the transmitted beam, (e)–(h) the CL (XP) component of the transmitted beam. The amplitude of the total transmitted field (is not shown here) is similar to the DP component but influence of the presence of half-moon in the XP component is also visible.

is unexpected (at first glance). Secondly, in the cross-polarization component, the spectral ring in (g) shows its half-part of decreased intensity, for $\vartheta_i < \Theta_i = \Theta_C$. This is result of lower branch for $\vartheta_i < \Theta_C$ in $|t_{XP}|$. Corresponding to this distorted spectral field there exist deformed spatial field, (e)–(f). In the center of the beam there are three "mini" vortices. Moreover, if we look closer to the amplitude and phase

of the direct polarization component, a) and b) respectively, we will also see three "mini" vortices. Note that number of the splitted vortices (in XP and DP component) is the same as the value of topological charge of the incident beam. Still, the total amount of the topological charge of the new vortices is in accordance with the topological charge of the incident beam.

3.4. Above critical incidence. We now chose specific angle of incidence equal to $55°$. All the spectral components correspond here to TIR. Moreover, the angle is chosen such that the differentiation $\partial_{k_\perp}$ of $|t_{XP}|$ and $|t_{DP}|$ be $\cong 0$, see Figs. 10 and 2.

a)

b)

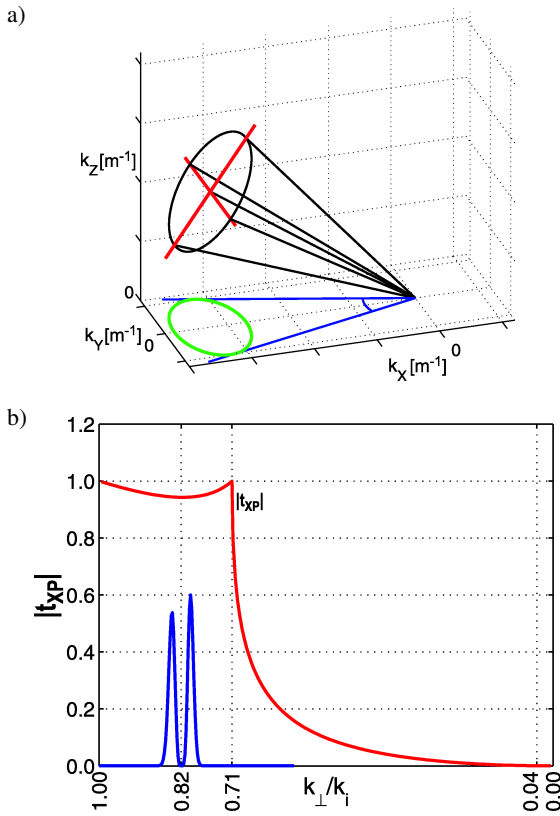Fig. 10 (colour online). Spectral cone in the case of oblique incidence ($\Theta_i = 55°$) (a), and magnitude of t_{XP} in the spectral domain (red solid curve) with the ring of the incident ELG beam $p = 1$, $l = 3$, $k_i w_w = 10 \cdot 2\pi$ (blue solid curve) (b). Meanings of the lines and curves are the same as in Fig. 4. The cone is inclined and the spectral ring peaks are shifted by $\sin(\Theta_i = 55°)$. Note that the range of azimuthal angles is less then $(-\pi/2, \pi/2)$, see blue circular sector in (a).

Under oblique incidence the action of the interface is qualitatively different in comparison with the action in the cases of "normal" incidence or the "significant" incidence. The range of the azimuthal angle is narrow enough so we can rewrite the transmission matrix, Eq. (3), in the approximate form

$$\underline{\underline{t}}_{(R,L)}^{\Theta_i > \Theta_S} \approx +t_{DP} \begin{bmatrix} 1 & 0 \\ 0 & 1 \end{bmatrix} + t_{XP} \begin{bmatrix} 0 & 1 - 2i\varphi \\ 1 + 2i\varphi & 0 \end{bmatrix}.$$

(10)

Therefore Eq. (10) suggests that field decomposition in its opposite polarization component will be of the similar shape as that of the incident beam. Compare Fig. 11 with Fig. 3. Domination of geometrical optics is clearly visible.
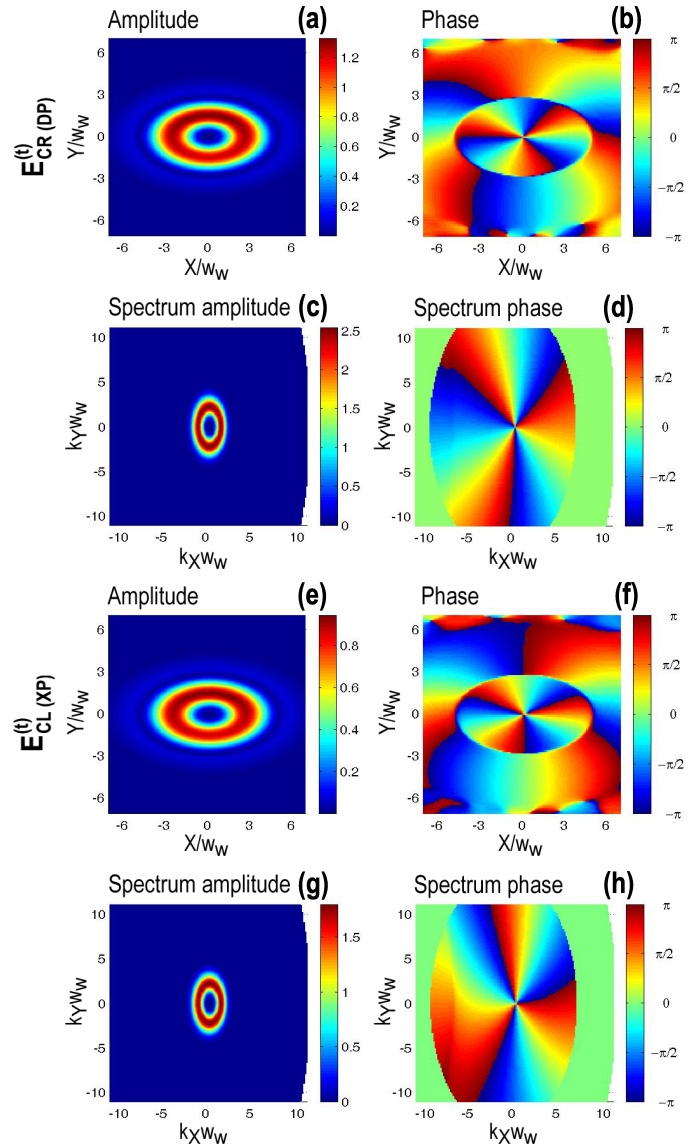

Fig. 11 (colour online). Transmitted components of the CR incident ELG beam $p = 1$, $l = 3$, $k_i w_w = 10 \cdot 2\pi$ (see Fig. 3) in the case of the oblique incidence ($55°$). The two first (second) rows show the DP (XP) component of the transmitted beam. The first and second column are respectively the amplitude and phase decompositions in the spatial and spectral domains. The third and fourth rows show the amplitude and phase of the spectral components. Values on the axis of abscissa are shown with reference to the global shift $k_i w_w \sin \theta_i$. (a)–(d) the CR (DP) component of the transmitted beam, (e)–(h) the CL (XP) component of the transmitted beam, domination of the geometrical optics is clearly visible. The amplitude of the total transmitted field (is not shown here) is similar to the DP (or XP) component.

4. Conclusions

In this contribution, we show that the "significant" boundary between two ranges of incident angle exists for the ELG beam

incidence. The first range represents roughly the normal incidence with the clearly visible excitation or annihilation of optical vortices in the opposite beam component. The second range represents the oblique incidence with the domination of the geometrical optics in the opposite component. The boundary between two regions of incidence is specified within the range where azimuthal angles decrease sharply. The angle of incidence that correspond to this "significant" case is decreasing with increasing of the width of the beam.

In the case of oblique incidence the range of azimuthal angles are narrower than in the "significant" or "normal" cases. Moreover, it is decreasing with growing of the incident angle or beam width at the waist. Narrow range of azimuthal angles finally results in the domination of the g-o contribution in the opposite beam component. However, in the case of critical incidence, 3D counterparts of the standard Fresnel coefficients possess singularities that peculiarly distort the beam spectral components and split the central optical vortex appeared in the spatial domain. Still, the phenomenon of vortex splitting is the characteristic feature of non-paraxial ELG beams incident obliquely on the interface [13].

Appendix A.

A note about the excitation of optical vortices in the case of normal incidence

For different polarization of the incident ELG beam, with radial p and azimuthal l indices, the excitation of optical vortices in the opposite transmitted component is different. Change of the topological charge l and radial index p is given by Eqs. (7), (8). The azimuthal index l increases (decreases) by 2, whereas radial index p decreases (increases) by 1 for CR (CL) incident beam polarization [5].

Some hint, that makes definition of t_{XP} more convenient, can be inferred from the case of normal incidence. In this case within the definitions of the ELG beams used in this paper there is some arbitrariness in the definitions of t_{XP} in the term $t_{XP}\widetilde{G}_{p\mp1,l\pm2}$. We can apply as well another definition of t_{XP} which entails the change of the form of $\widetilde{G}_{p\mp1,l\pm2}$. In order to make the modified spectral coefficient t_{XP} approximately constant at and near the centre of the spectrum ($k_X = 0$, $k_Y = 0$), we have to multiply it by some spectral normalization term. Note that t_{DP} is roughly constant in this region, see Fig. 2. Coefficient t_{XP} possesses dependence $\sim k_\perp^2$ in the centre. If we consider this, the normalization term will be $\sim 1/k_\perp^2$. Note that, $2\kappa\bar{\kappa}/k_\perp^2 = 1$. Let put this unity after t_{XP} in Eqs. (7) and (8). Now, using Eq. (5) with $\kappa\bar{\kappa}$ instead of $\kappa^{p+l}\bar{\kappa}^p$ we can write:

$$\kappa\bar{\kappa}\widetilde{G}_{p,l}^{(EL)}(\kappa,\bar{\kappa},Z) = -w_w^{-2}\widetilde{G}_{p+1,l+0}^{(EL)}(\kappa,\bar{\kappa},Z). \quad (11)$$

Considering presence of $-w_w^{-2}$ the constant t_{XP} can be given by:

$$-2t_{XP}(w_w k_\perp)^{-2} \equiv t'_{XP}. \quad (12)$$

Using last two equations above we can rewrite action of the interface as:

$$\begin{bmatrix} \widetilde{E}_R^{(t)} \\ \widetilde{E}_L^{(t)} \end{bmatrix}_{CR} = t_{DP}\begin{bmatrix} \widetilde{G}_{p,l}^{(EL)} \\ 0 \end{bmatrix} + t'_{XP}\begin{bmatrix} 0 \\ \widetilde{G}_{p+0,l+2}^{(EL)} \end{bmatrix}, \quad (13)$$

$$\begin{bmatrix} \widetilde{E}_R^{(t)} \\ \widetilde{E}_L^{(t)} \end{bmatrix}_{CL} = t_{DP}\begin{bmatrix} 0 \\ \widetilde{G}_{p,l}^{(EL)} \end{bmatrix} + t'_{XP}\begin{bmatrix} \widetilde{G}_{p+2,l-2}^{(EL)} \\ 0 \end{bmatrix}. \quad (14)$$

Note that the identical form of t'_{XP} can be given for the Elegant Hermite-Gaussian beams analyzed in Ref. [5].

REFERENCES

[1] W. Nasalski, *Optical Beams at Dielectric Interfaces – Fundamentals*, Institute of Fundamental Technological Research Polish Academy of Sciences, Warszawa, 2007.

[2] L. Allen and M.J. Padgett, and M. Babiker, "The orbital angular momentum of light", *Progress in Optics* 39, 291–372 (1999).

[3] A.T. O'Neil, I. MacVicar, L. Allen, and M.J. Padgett, "Intrinsic and extrinsic nature of the orbital angular momentum of a light beam", *Phys. Rev. Lett.* 88, 053601 (2002).

[4] J. Leach, J. Courtial, K. Skeldon, S.M. Barnett, S. Franke-Arnold, and M.J. Padgett, "Interferometric methods to measure orbital and spin, or the total angular momentum of a single photon", *Phys. Rev. Lett.* 92, 013601 (2004).

[5] W. Nasalski, "Polarization versus spatial characteristics of optical beams at a planar isotropic interface", *Phys. Rev. E* 74, 056613 (2006).

[6] W. Nasalski and Y. Pagani, "Excitation and cancellation of higher-order beam modes at isotropic interfaces", *J. Opt. A: Pure Appl. Opt.* 8, 21–29 (2006).

[7] A.E. Siegman, "Hermite-gaussian functions of complex argument as optical-beam eigenfunctions", *J. Opt. Soc. Am.* 63, 1093–1094 (1973).

[8] A.E. Siegman, *Lasers*, University Science Books, Mill Valley, 1986.

[9] J. Enderlein and F. Pampaloni, "Unified operator approach for deriving Hermite-Gaussian and Laguerre-Gaussian laser modes", *J. Opt. Soc. Am. A* 21, 1553–1558 (2004).

[10] F. Gori, G. Guattari, and C. Padovani, "Bessel-Gauss beams", *Opt. Commun.* 64, 491–495 (1987).

[11] F.I. Baida, D. Van Labeke, and J-M. Vigoureux, "Numerical study of the displacement of a threedimensional Gaussian beam transmitted at total internal reflection. Near-field applications", *J. Opt. Soc. Am. A* 17, 858–866 (2000).

[12] W. Nasalski, "Three-dimensional beam reflection at dielectric interfaces", *Opt. Commun.* 197, 217–233 (2001).

[13] W. Nasalski, "Elegant vector normal modes at a dielectric interface", ArXiv. 0810.2291, (2008).